Electronic Supplementary Material (ESI) for Materials Horizons.
This journal is © The Royal Society of Chemistry 2018

Supporting Information for Manuscript Entitled with

A smart hemicapsule with multiple dynamic functions

Chi-An Chen, Chia-Chen Li* and Chih-Hsien Chen

Department of Materials & Mineral Resources Engineering, and Institute of Materials Science and Engineering, National Taipei University of Technology, Taipei 10608, Taiwan

* Correspondence author. E-mail: ccli@ntut.edu.tw

1. Materials and methods

Raw Materials: Urea (99%, Showa, Japan), formaldehyde (37%, Echo, Taiwan), resorcinol (98%, Acros, USA), ammonium chloride (99.5%, Showa, Japan), triethanolamine (TEA; 99%, Sigma-Aldrich, USA), poly(ethylene-alt-maleic anhydride) (EMA; 99%, Sigma-Aldrich, USA), poly(methyl methacrylate) (PMMA; 99.5%, Acros, USA), polystyrene (PS; 99.5%, Acros, USA), and sodium dodecyl sulfate (SDS; 99%, Acros, USA) were the reagents used for the synthesis of the hemicapsule. An oil-soluble red dye (Orimax Red 308, Orient Chemical Ltd., Korea) was used for the coloring of the solid part of the hemicapsules. The chemical reagents used for the dynamic test were Brilliant Blue (BB; <87%, MAP technologies, England) and Rhodamine B (R-B, >95%, Sigma, USA). The solvents used in this investigation include toluene (98%, Acros, USA), glacial acetic acid (99.8%, Scharlau, Spain), ethanol (95%, Echo, Taiwan), acetone (99.5%, Echo, Taiwan), and deionized water. A standard PBS solution was prepared by mixing 137 mmol L^{-1} of sodium chloride (NaCl; 99.5%, Showa, Japan), 2.7 mmol L^{-1} of potassium chloride (KCl; 99%, Shimakyu's Pure Chemicals, Japan), 10 mmol L^{-1} of sodium phosphate (Na_2HPO_4; 95%, Acros, USA), and 1.8 mmol L^{-1} potassium phosphate (KH_2PO_4; 99%, J.T. Baker, USA). Aqueous solutions of NaOH and hydrochloride (HCl; 12 M, Sigma-Aldrich, Australia) were used for pH adjustments.

Fabrication of Hemicapsules: The hemicapsules were synthesized by two simple steps. In the first step, Janus particles were fabricated by dissolving 0.19 g of PMMA and PS, respectively, in 5 ml toluene, and the toluene solution was emulsified into an aqueous solution containing 0.3 wt% of SDS using a homogenizer (T25, IKA, Germany) at 3400 rpm for 2 min. Next, the emulsion was heated to 55 °C and stirred for an additional 2 h to evaporate toluene and precipitate the Janus particles. The particles were removed from the suspension and washed repeatedly using deionized water. To prepare magnetic Janus particles, the aforementioned 5 mL toluene was replaced by a 5 mL toluene suspension containing commercial nano-Fe_3O_4 (97%, Alfa Aesar, USA) before the additions of PS and PMMA. In the second step, *in situ* polymerization of PUF was performed on the Janus particles. The Janus particles (0.38 g) were mixed with 1.25 g urea, 0.125 g resorcinol, 0.125 g ammonium chloride, and 3.16 g formaldehyde in 100 ml deionized water, and the pH of the solution was adjusted to 3.5 by the addition of TEA and warmed to 40 °C to start the polymerization for 2 h. After the reaction, the product was washed with deionized water several times. Next, the PMMA-half of the Janus particle inside the PUF shell was removed by immersing in glacial acetic acid at room temperature for 12 h. For the handcrafted microchannel, it was fabricated by sculturing a plastic insulation tape with a thickness of 150 μm on a glass (Fig. S6).

Characterizations: The microstructure of the synthesized hemicapsule was observed using a transmission electron microscope (TEM; JEM-2100F, Jeol, Japan), a field-emission scanning electron microscope (FE-SEM; S-470, Hitachi, Tokyo, Japan), an optical microscope (OM; Primo Star, Zeiss, Jena, Germany), and a confocal fluorescence microscope (Leica TCS SP8, Leica Microsystems, Wetzlar, Germany). The confocal fluorescence microscopy images were taken using a 561 nm (1.5 mW) white light laser. The hemicapsule suspension was dropped in a glass microscope dish and was measured in an acidic solution of pH1. The optical sections were gathered in 0.5-μm steps perpendicular to the microscope optical axis, and 4 of 20 images were collected and presented in the main article (individual images are separated by a distance of approximately 2 μm). The particle size distribution of the synthesized hemicapsule was measured by light scattering method (V-630, JASCO, Germany). The chemical composition and surface chemistry of the hemicapsule were characterized by Fourier transform infrared (FT-IR) spectroscopy (DA 8.3, Bomen, Canada), X-ray diffraction (XRD; D2 Phaser, Bruker, MA, USA), thermal gravimetric analysis (Q50, TA instruments Ltd., Crawley, UK), and the electroacoustic method (ZetaProbe, Colloidal Dynamics Inc., MA, USA). In the electro-stimulus release experiment, a power supplier (PST-3030D, GW Instek, Taiwan) was used to generate an electric field. The concentration of dyes was determined quantitatively using ultraviolet and visible (UV-Vis) absorption spectroscopy (V-630, Jasco, Japan).

2. Supplementary figures

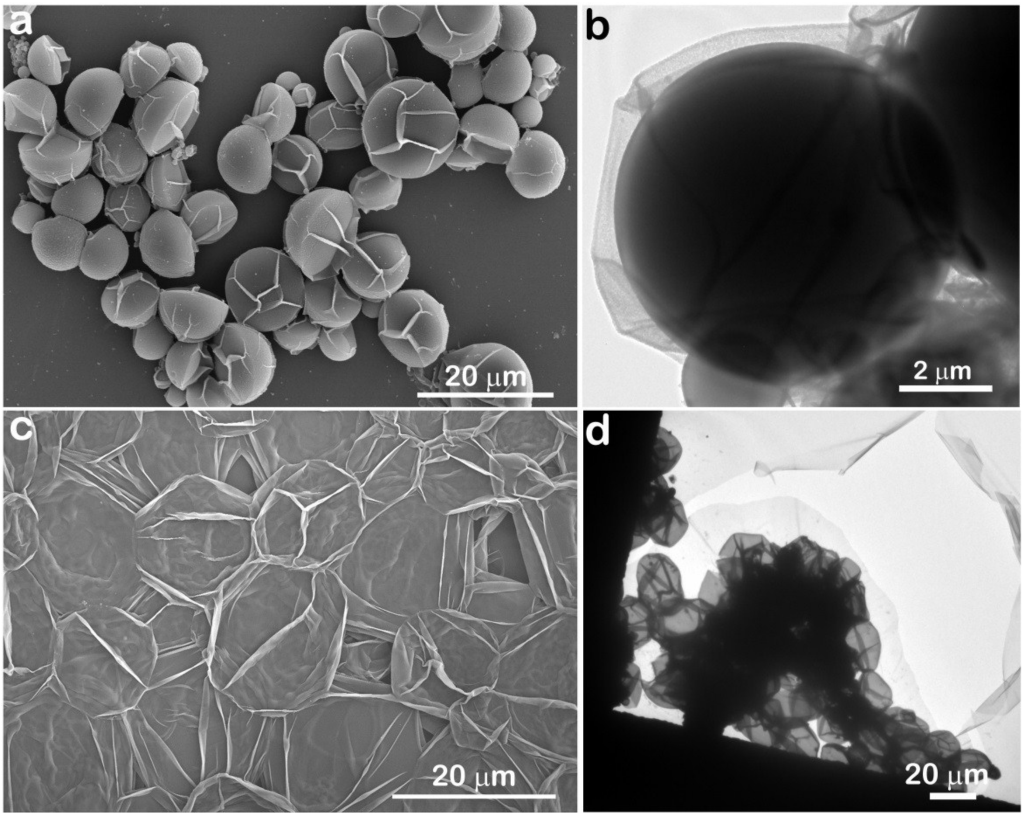

Fig. S1 (a) SEM and (b) TEM images of the dried hemicapsules. (c) SEM and (d) TEM images of dried hollow capsules without the half-sphere support.

The importance of the half-sphere design for the bracing of the dried structure is obvious from the comparison of Fig. S1(a,b) with Fig. S1(c,d). Without the half-sphere, the capsule structure collapsed and flattened after drying. Because the flattened capsules provide greater contact areas, severe stacking and flocculation occur among them, rendering the reversal of the morphology of the dried capsules to their original morphology before drying when re-dispersed into a liquid phase impossible.

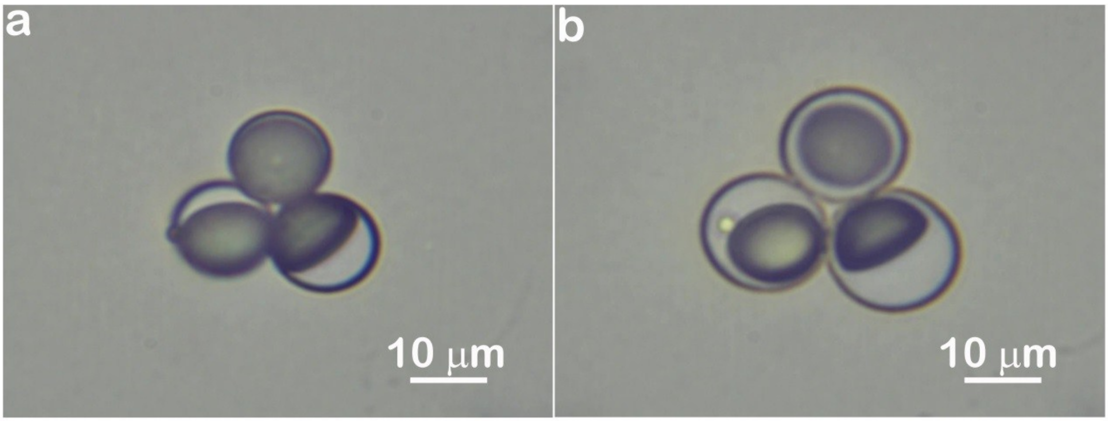

Fig. S2 (a) Morphology of the hemicapsules in water with unadjusted pH6 (the original pH of deionized water). (b) Morphology of the inflated hemicapsules at pH11.

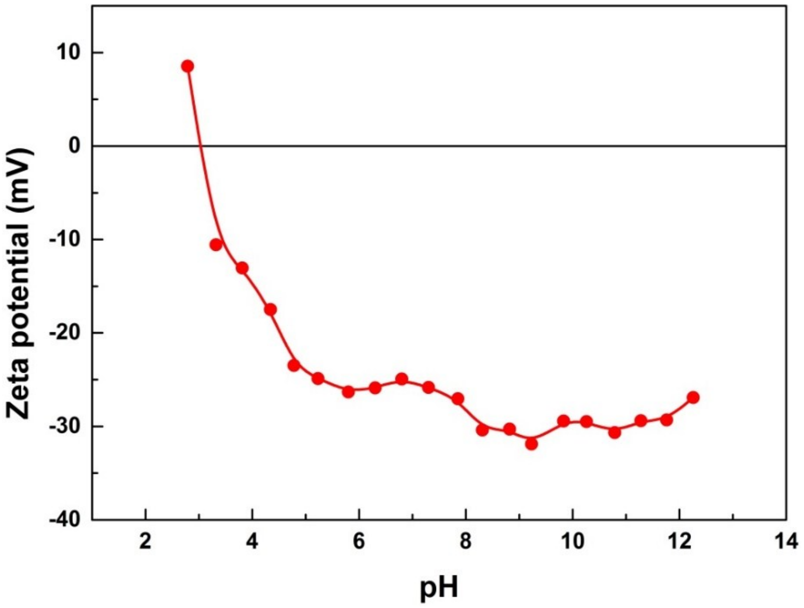

Fig. S3 The zeta potentials of 0.2 wt% hemicapsule in water, as a function of pH.

The hemicapsule shows an IEP at around pH2-3, indicating that the hemicapsule is negatively charged at pH > 2-3 and positively charged at pH < 2-3.

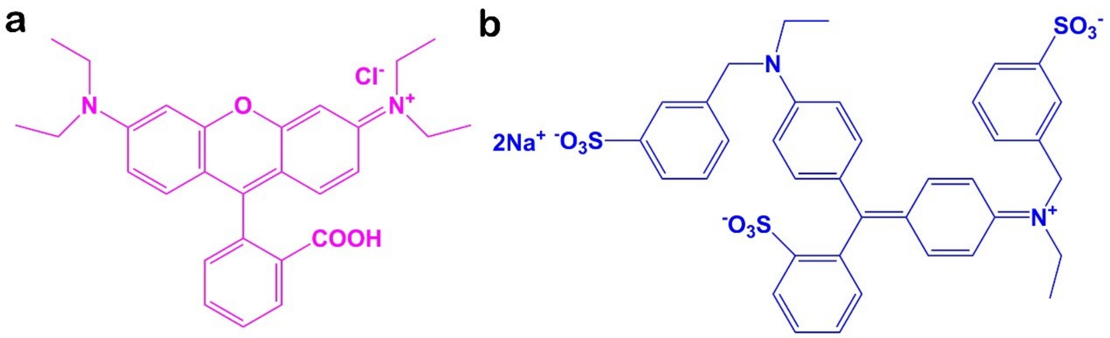

Fig. S4 Chemical structures of (a) Rhodamine B (R-B) and (b) Brilliant Blue (BB).

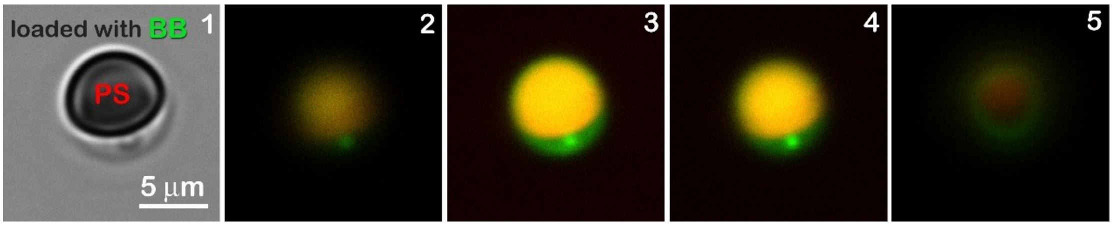

Fig. S5 Fluorescence confocal microscopy (FCM) photograph showing sections of the BB-loaded hemicapsule; the photograph denoted 1 is the bright-field image and those photos denoted 2-5 are the FCM images from the sectioned planes separated by a distance of approximately 1 μm.

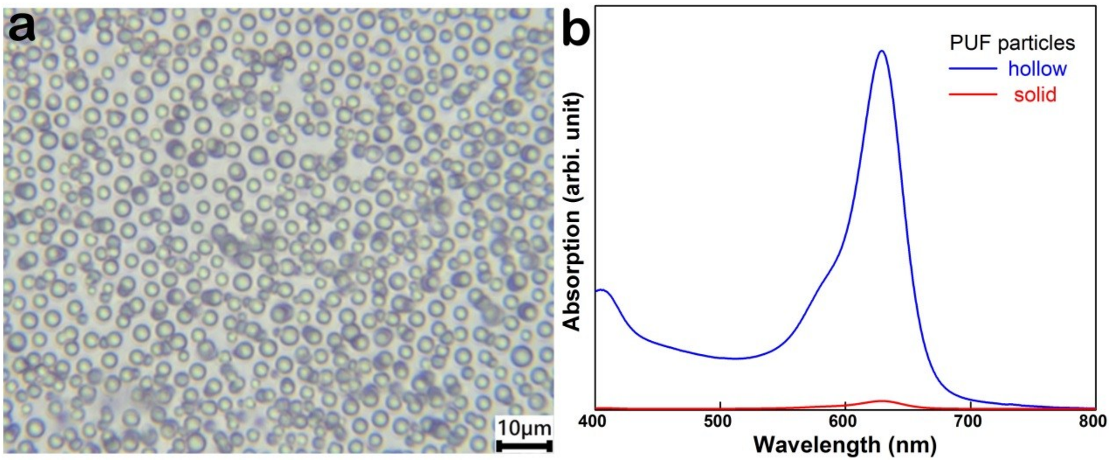

Fig. S6 (a) OM photograph of the synthesized solid PUF particle: the particle size is ranged from 2-5 μm. (b) UV-Vis spectra of the aqueous solutions of BB leaked from the same amount of BB-loaded hollow and solid PUF particles.

The PUF hollow particle for the further experiment in Fig. S6 was obtained by dissolving the PS half of the hemicapsule using toluene. For the synthesis of the solid PUF particle, 0.5 g of urea, 0.05 g of ammonium chloride, 0.05 g resorcinol, 1.27 g of formaldehyde, and a 5 mL of 10 wt% EMA were mixed in a 45 mL deionized water. Then, the pH of the above solution was adjusted to 3.5 by the addition of TEA and warmed to 40 °C to start the polymerization for 2 h. After the reaction, the product was washed with deionized water several times, which the resulted particle morphology is shown in Fig. S6(a).

For the experiment in Fig. S6(b), the same amount of hollow and solid PUF particles were respectively immersed in aqueous solutions of 125 ppm BB with pH1. After immersion for 48 h, both particle samples were transferred into a fresh water with pH11 for a complete releasing of BB for 72 h; the released amount is assumed to approximate the loading capacity of the particles and can be measured by UV-Vis spectroscopy. Notably, the complete releasing of the hollow and solid PUF particles has to be confirmed before the above measurement. The confirmation was done by releasing again of the already-released particles in another fresh water with pH11, and then the residue in the solution was characterized by UV-Vis spectroscopy. In the result of Fig. S6(b), it is apparent that the hollow particle contains a much higher amount of BB than the solid particle, evidencing the improved loading capacity due to the hollow structure.

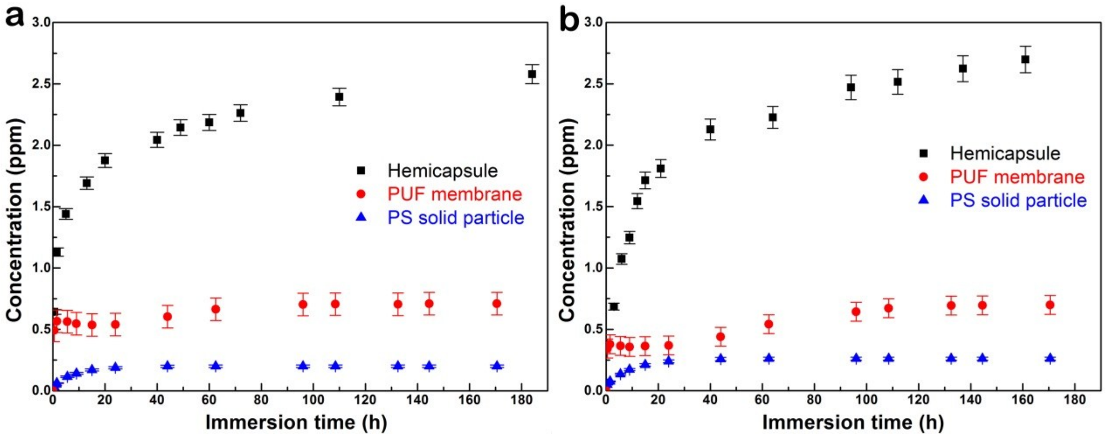

Fig. S7 Adsorption amounts of (a) R-B and (b) BB in hemicapsule, PUF membrane, and PS solid particle, as a function of immersion time. The concentration of the dye solutions is 10 ppm and the pH is 1.

In the experiment of Fig. S7, the further analyses of the adsorption kinetics of the dyes at the PUF membrane and PS solid particle were conducted, and the results were compared with that of the dyes at the hemicapsule. For measuring the adsorption of the dyes at the PUF membrane, two types of particles, including the PUF-encapsulated PS particle (PUF@PS particle) and the PS solid particle, were adopted instead of directly experimenting the PUF hollow particle, which is because the adsorption amount of the PUF hollow particle will be dominated by the hollow chamber rather than by its membrane, as has evidenced in Fig. S6.

The PS solid particle was fabricated by dissolving 0.15 g of the commercial PS powder in 1.8 mL toluene, and then emulsifying the PS solution in 45 mL deionized water containing 0.15 g SDS using a homogenizer at 3400 rpm for 2 min. Next, the emulsion was heated to 60 °C and stirred for 2 h to evaporate toluene and precipitate the PS particles, and the particles were washed repeatedly using deionized water. For the PUF@PS particle, it was synthesized using the same initial steps for the synthesis of the hemicapsule, except the core material is the PS particle in this reaction.

Assume that the adsorption of the dyes at the membrane of PUF@PS will not be affected by the adsorption of its PS interior; the adsorption amounts of R-B and BB at the PUF membrane can be roughly calculated by subtracting the adsorbed amount of PUF@PS by that of PS solid particle. Fig. S7(a) shows the adsorption amounts of R-B, as a function of immersion/adsorption time, for the hemicapsule (data are from Fig. 4(c)-(d)), the PUF membrane (data are from above calculation/subtraction), and the PS solid particle. Note that the concentration presented at the y-axis is the reduced concentration of the dye in the bulk solution due to being absorbed by the three different particles. It is observable that the adsorption amount is much higher for the hemicapsule than for the PUF membrane or the PS solid particle, indicating the great contribution of the hollow structure to the large capacity of the hemicapsule. A similar result was also obtained for the adsorptions of BB for the three types of particles, as shown in Fig. S7(b). Moreover, it is clear to see that the adsorption of the dye for the hemicapsule occurs at almost the same time as the dye adsorbing at the PUF membrane. Nevertheless, the adsorption of the dyes at the PUF membrane reaches saturation rapidly, which is different from the adsorption kinetics of the dyes for the hemicapsule. The adsorptions of the dyes for the hemicapsule shown in Fig. S7(a)-(b) reveal a typical behavior of diffusion, so the dyes should be loaded into the hemicapsule through a diffusion mechanism. Furthermore, the adsorption behavior of the dyes for the PS solid particle is similar to the adsorption for the hemicapsule but just in a much lower adsorbed concentration.

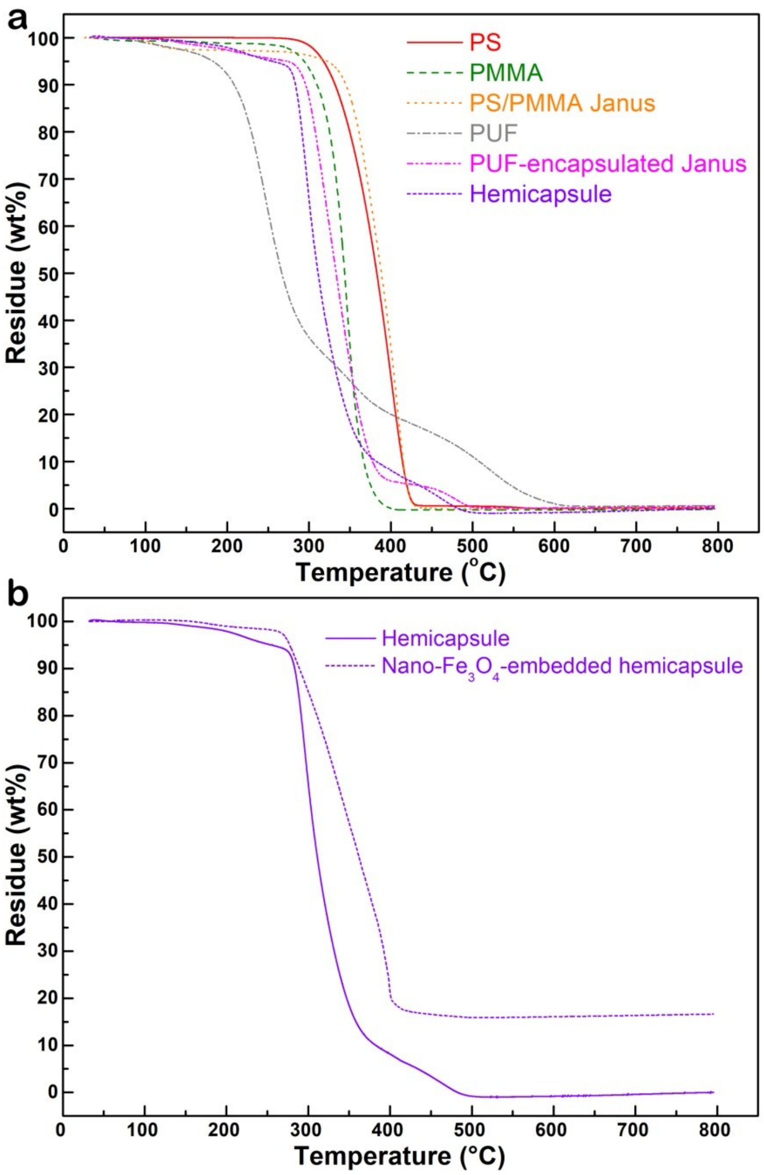

Fig. S8 Thermal gravimetric analysis for characterizations of (a) PS, PMMA, PS/PMMA Janus particle, PUF, PUF-encapsulated Janus particle and hemicapsule, and (b) hemicapsule and nano-Fe_3O_4-embedded hemicapsule.

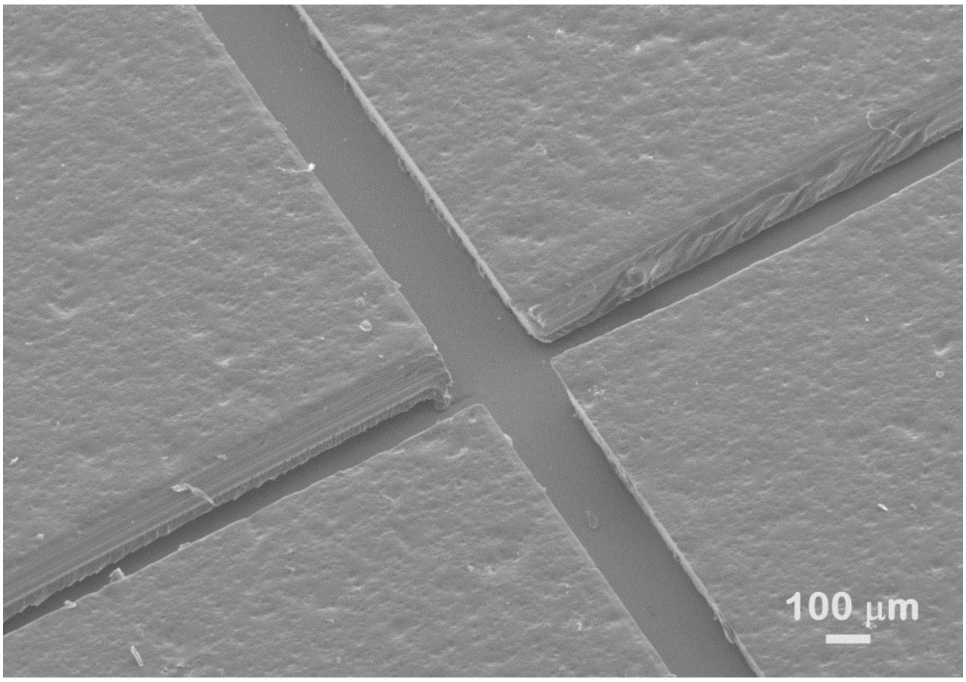

Fig. S9 SEM image of the handcrafted microchannel.